FEBS Letters 581 (2007) 1275–1286

Characterisation of cyclin D1 down-regulation in coronavirus infected cells

Sally M. Harrison[a], Brian K. Dove[a], Lisa Rothwell[b], Pete Kaiser[b], Ian Tarpey[c], Gavin Brooks[d], Julian A. Hiscox[a,e,*]

[a] *Institute of Molecular and Cellular Biology, Faculty of Biological Sciences, University of Leeds, Leeds, LS2 9JT, UK*
[b] *Institute for Animal Health (Compton Laboratory), UK*
[c] *Intervet UK Ltd., Milton Keynes, UK*
[d] *School of Pharmacy, University of Reading, Reading, UK*
[e] *Astbury Centre for Structural Molecular Biology, University of Leeds, Leeds, UK*

Received 3 November 2006; revised 30 January 2007; accepted 13 February 2007

Available online 28 February 2007

Edited by Hans-Deiter Klenk

Abstract The positive strand RNA coronavirus, infectious bronchitis virus (IBV), induces a G2/M phase arrest and reduction in the G1 and G1/S phase transition regulator cyclin D1. Quantitative real-time RT-PCR and Western blot analysis demonstrated that cyclin D1 was reduced post-transcriptionally within infected cells independently of the cell-cycle stage at the time of infection. Confocal microscopy revealed that cyclin D1 decreased in IBV-infected cells as infection progressed and inhibition studies indicated that a population of cyclin D1 could be targeted for degradation by a virus mediated pathway. In contrast to the SARS-coronavirus, IBV nucleocapsid protein did not interact with cyclin D1.

Keywords: Coronavirus; Infectious bronchitis virus; IBV; Cyclin D1; Cell cycle; Taqman; Regulation

1. Introduction

The ordered growth and division of cells is described as the cell cycle, which can be separated into a number of distinct phases, gap 1 (G1), synthesis (S), gap 2 (G2) and mitosis (M) [1] followed by cytokinesis [2]. Each stage of the cell cycle is regulated and controlled by both positive and negative regulators, for example cyclins and their partner molecules, the cyclin dependent kinases (CDKs) and associated inhibitor complexes (CDKIs) [3]. Many viruses interact with the cell cycle to promote favourable conditions for virus infection and for disrupting host cell proliferation and function [4]. However, the alteration of the host cell cycle by RNA viruses has not been described as extensively when compared to DNA or retroviruses.

Coronaviruses are a family of positive strand RNA viruses which replicate in the cytoplasm of infected cells and belong to the order *Nidovirales* [5]. Infection of cells with the avian coronavirus infectious bronchitis virus (IBV) causes a G2/M phase arrest [6], with changes in the amounts of proteins involved in cell cycle regulation, such as a reduction in cyclin D1 [6]. In the case of the murine coronavirus, mouse hepatitis virus (MHV), infection results in an arrest in the G0/G1 phase of the cell cycle with a resulting decrease in the D-type cyclins [7]. Over-expression studies indicated that a component of the viral replicase could arrest cells in this phase of the cell cycle [8]. On the other hand, in patients infected with severe acute respiratory syndrome (SARS) coronavirus hepatocytes have been reported to accumulate in mitosis [9] and this is in contrast to a number of SARS-coronavirus proteins that when over expressed lead to an accumulation of cells in the G0/G1 phase of the cell cycle [10,11]. For example, the SARS-coronavirus nucleocapsid (N) protein has been reported to block S phase progression [12] and prolong the G0/G1 phase and shorten the S phase [13]. Likewise, when over expressed the IBV N protein delays cell growth and results in aberrant cytokinesis [14,15], which is also observed in infected cells [6,15].

Cyclin D1, when complexed with either CDK 4 or 6, positively regulates progression of cells through the G1-S phase of the cell cycle. Like all cyclins, levels of cyclin D1 fluctuate depending on the particular stage of the cell cycle, with levels of cyclin D1 accumulating in the G1 phase. Cyclin D1 is then rapidly degraded via the cellular proteosome during S phase allowing DNA synthesis to occur [16]. Levels then begin to rise again during the G2 and M phases of the cell cycle. Regulation of cyclin D1 expression is controlled by the abundance of cyclin D1 mRNA, sub-localisation and degradation [17]. In this study the reduction of cyclin D1 was investigated in IBV infected cells.

2. Materials and methods

2.1. Cells and viruses

The growth and titration of IBV Beaudette-US, an embryo-adapted IBV strain [18], and the growth of Vero cells were performed as described previously [6]. Cell culture experiments were performed within sub-confluent cells to avoid artefact G0/G1 populations due to contact inhibition and in the absence of antibiotic or anti-fungal agents. Cells were infected with IBV at 2×10^6 pfu/ml ($\sim$MOI = 1) at 70% confluent and incubated for 1 h at 37 °C, after which the virus was replaced with cell growth media. UV inactivation of IBV was performed as described previously [6].

*Corresponding author. Address: Institute of Molecular and Cellular Biology, Faculty of Biological Sciences, University of Leeds, Leeds, LS2 9JT, UK. Fax: +44 0 113 343 3167.
E-mail address: j.a.hiscox@leeds.ac.uk (J.A. Hiscox).

0014-5793/$32.00
doi:10.1016/j.febslet.2007.02.039

2.2. Vero cell enrichment

Vero cells were cell-cycle enriched as described previously [6] by serum deprivation (G0), double thymidine treatment (G1/S) and nocodazole treatment (G2/M) [6]. The efficiency of cell cycle synchronisation was determined by flow cytometric analysis [6].

2.3. Treatment of cells with LiCl and MG132

Vero cells were seeded at 2×10^5 and grown to 70% confluency before being mock or IBV infected at 2×10^6 pfu/ml. At 8 h post infection the cells were treated with 10 μM MG132 or 0.5, 1, 2.5 or 5 mM LiCl or a combination of both where detailed. At 24 h post infection the cells were lysed and total cellular protein quantified by BCA assay. Western blot analysis was then performed using antibodies against cyclin D1, GAPDH and IBV proteins. Alternatively, cells were fixed and made permeable for subsequent immunofluoresence analysis.

Table 1
Real time RT-PCR analysis of IBV genomic RNA levels during a 24 h infection in Vero cells as shown by corrected 40-C_t values

Time post-infection (h)	Correct 40-C_t values
0	0
1	12.704 ± 0.391
4	10.336 ± 0.045
8	14.545 ± 0.183
12	15.076 ± 0.119
24	16.068 ± 0.124

2.4. Leptomycin B (LMB) treatment of cells

Mock and IBV-infected Vero cells were treated with 2.5 ng/ml LMB at 1 h post infection. At 16 h post infection, cells were processed as appropriate either for Western blot or immunofluoresence analysis.

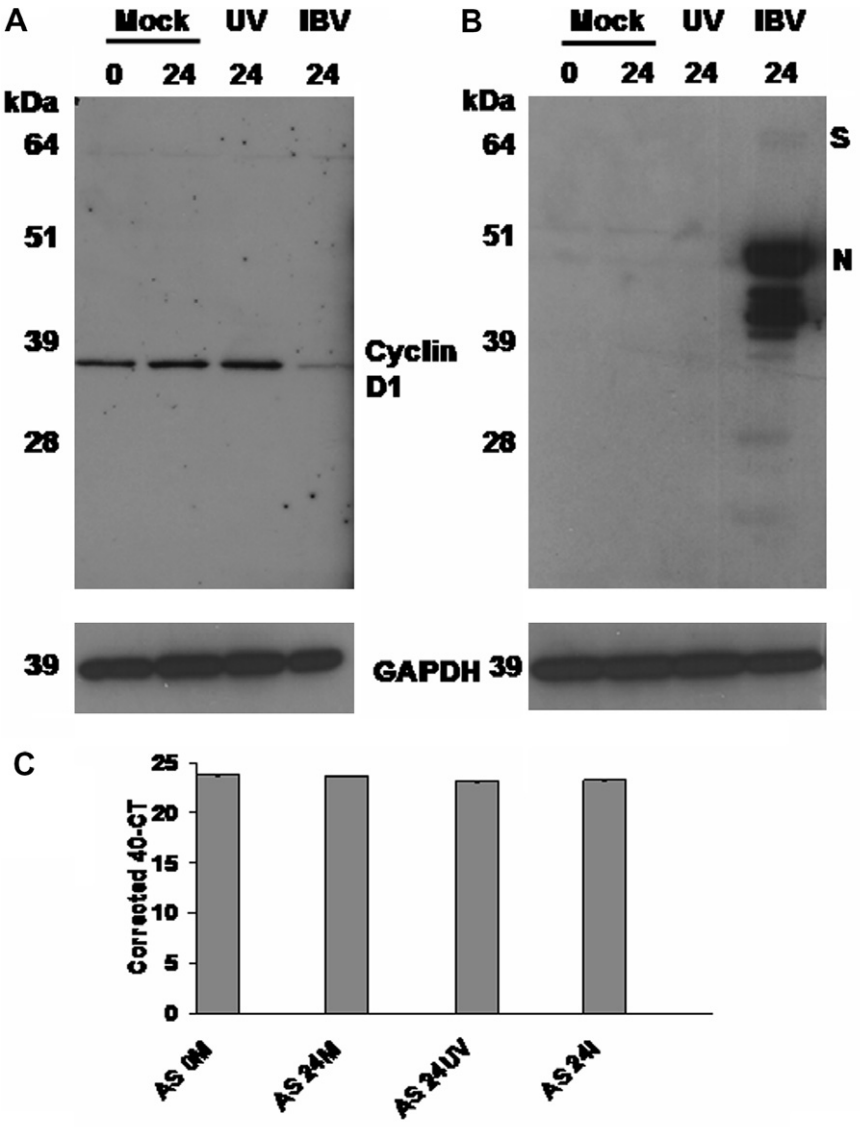

Fig. 1. Western blot analysis of cyclin D1 (A) and IBV proteins (B) in mock-infected (mock) or cells infected with IBV (IBV) or treated with UV-inactivated IBV (UV). Time post infection is indicated above the respective lane and the migration of molecular weight markers is indicated to the left. Equal protein loading was confirmed by Western blot analysis of GAPDH. The data shown is one of three separate experiments. (C) TaqMan analysis of the amount of cyclin D1 mRNA at the indicated times (h) in asynchronously (AS) replicating cells either mock (M) or infected with IBV (I) or treated with UV-inactivated virus (UV).

LMB activity was shown using a previously described luciferase assay [19] and carried out in triplicate.

2.5. Transient cell transfection and plasmids

Vero cells were cultured in six well plates until 70% confluent, then transfected with 1 μg of plasmid DNA using Lipofectamine transfection reagent (Invitrogen). The constructs utilised in this study, pEGFP-IBVN or PEGFP-IBVN$_{\Delta NES}$, were used for the expression of either wild type N protein or N protein in which nuclear export signal has been deleted, are fused to EGFP [20–22]. The ECFP-cyclin D1 fusion protein expression plasmid, pECFP-cyclin D1 was constructed by amplifying human cyclin D1 from a Gateway Destination Vector (pEXP1-dest) (Invitrogen) containing cyclin D1, using the following primers which incorporated a *Sac*II and *Xho*I restriction: Forward: 5′ GGAATATTCTCGAGCGATGGAACACCAGCTC 3′ and Reverse 5′ TTATTATTCCGCGGCTAGATGTCCACGTC 3′, before being ligated into pECFP-C1 (cyan fluorescent protein).

2.6. Western blot analysis

Mock, UV inactivated virus treated and IBV infected Vero cells were harvested 24 h post-infection and lysed with radioimmuoprecipitation (RIPA) buffer. Total protein was quantified by BCA assay (Promega) and 10 μg of total protein from each sample was analyzed by Western blot [6]. IBV proteins were detected with chicken anti-IBV polyclonal sera (1:20000, Charles River). Cyclin D1 was detected with a rabbit anti-cyclin D1 polyclonal antibody (1:500, Santa Cruz). Mouse anti-GAPDH (6C5) monoclonal antibody (1:40000, AbCam) was used to detect glyceraldehyde-3-phosphatedehydrogenase (GAPDH).

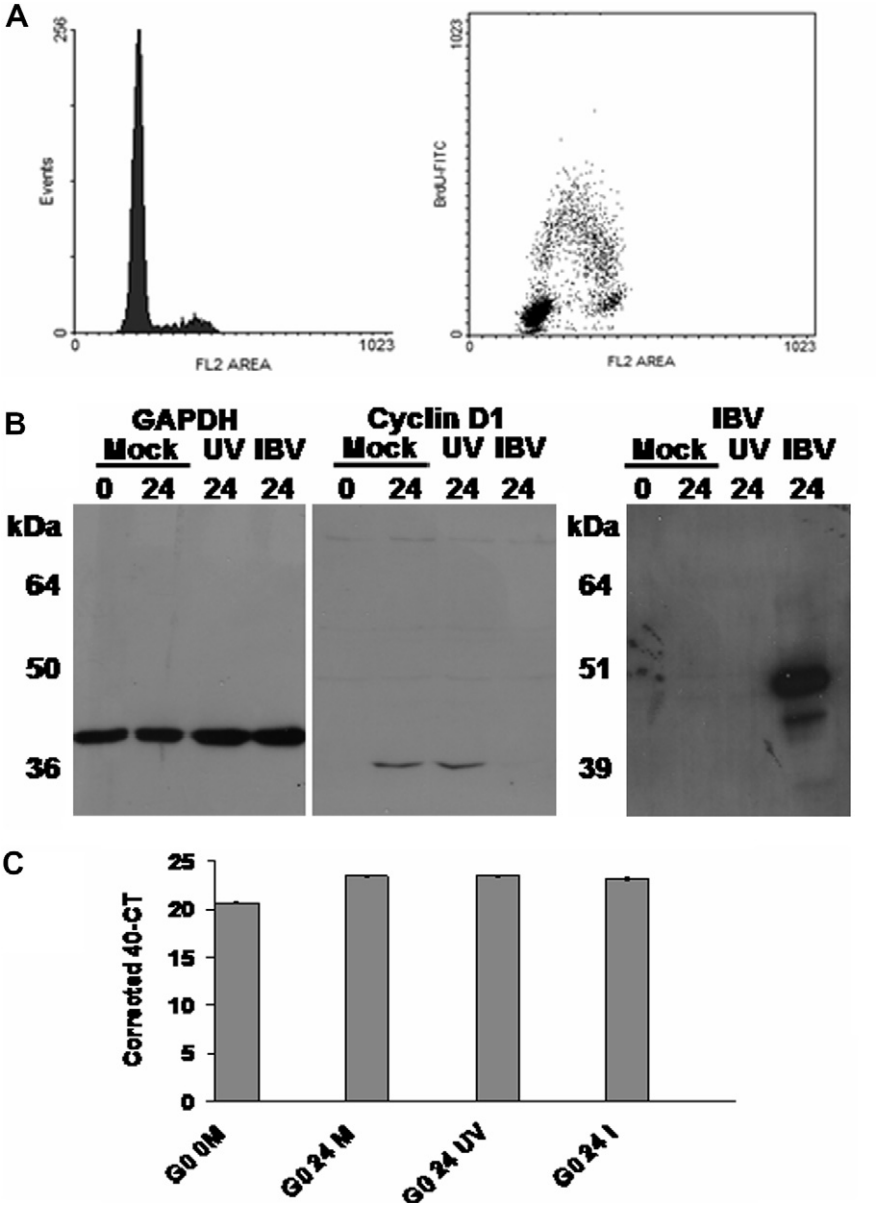

Fig. 2. (A) Propidium iodide (PI) plot and BrdU/PI staining of cell cycle profiles of cells enriched in the G0 phase of the cell cycle using serum starvation (for the latter plot the *X*-axis is the intensity of PI staining and the *Y*-axis is the intensity of BrdU staining). (B) Western blot analysis of GAPDH, cyclin D1 and IBV proteins in mock infected cells (Mock) and cells treated with UV-inactivated virus (UV) and infectious virus (IBV) at the times indicated post-infection (h) in cells enriched in the GO phase of the cell cycle and then released. The migration of molecular weight markers is indicated to the left. (C) TaqMan analysis of the amount of cyclin D1 mRNA in cells enriched in the G0 phase of the cell cycle (indicated G0) and then released at the indicated times (h), in either mock (M) or cells infected with IBV (I) or treated with UV-inactivated virus (UV).

2.7. Cellular RNA preparation

Total cellular RNA was extracted at 0 h and 24 h post-infection by the RNeasy method (Qiagen).

2.8. Taqman analysis of cyclin D1 mRNA

Cyclin D1 mRNA levels in mock, IBV infected and cells treated with UV-inactivated virus were quantified by TaqMan real time PCR. Primers and probes for both cyclin D1 and 28S were designed using the Primer Express software program (Applied Biosystems). Cyclin D1 forward primer: GTGAACAAGCTCAAGTGGAACCT; reverse primer: TGGCATTTTGGAAAGGAAGTG; probe: TGACCCCGCACGATTTCATCGA. 28S forward primer: GGCGAAAGACTAATCGAACCAT; reverse primer: CGAGAGCGCCAGCTATCCT; probe: TAGTAGCTGGTTCCCTCCGAAGTTTCCCT and experiments performed as described previously [23,24]. Where appropriate these probes were designed across exon–exon boundaries so no genomic DNA or unprocessed RNA would be amplified. IBV genomic RNA was quantified using previously describe primer/probe sets: forward primer: CGTACCGGTTCTGTTGTGTGA; reverse primer: GCCCAACGCTAGGCTCAA and probe: TCACCTCCCCCCACATACCTCTAAGGG [25]. Quantification was based on increased fluorescence detected due the 5′ exonuclease activity of the Taq DNA polymerase during PCR amplification hydrolysing the target specific probes. The reporter signal was normalised by the reference dye 6-carboxy-*c*-rhodamine, which was not actually involved in amplification. Results were expressed in terms of C_t values (threshold cycle value); the cycle at which the change in reporter dye passes a significance threshold (ΔR_n).

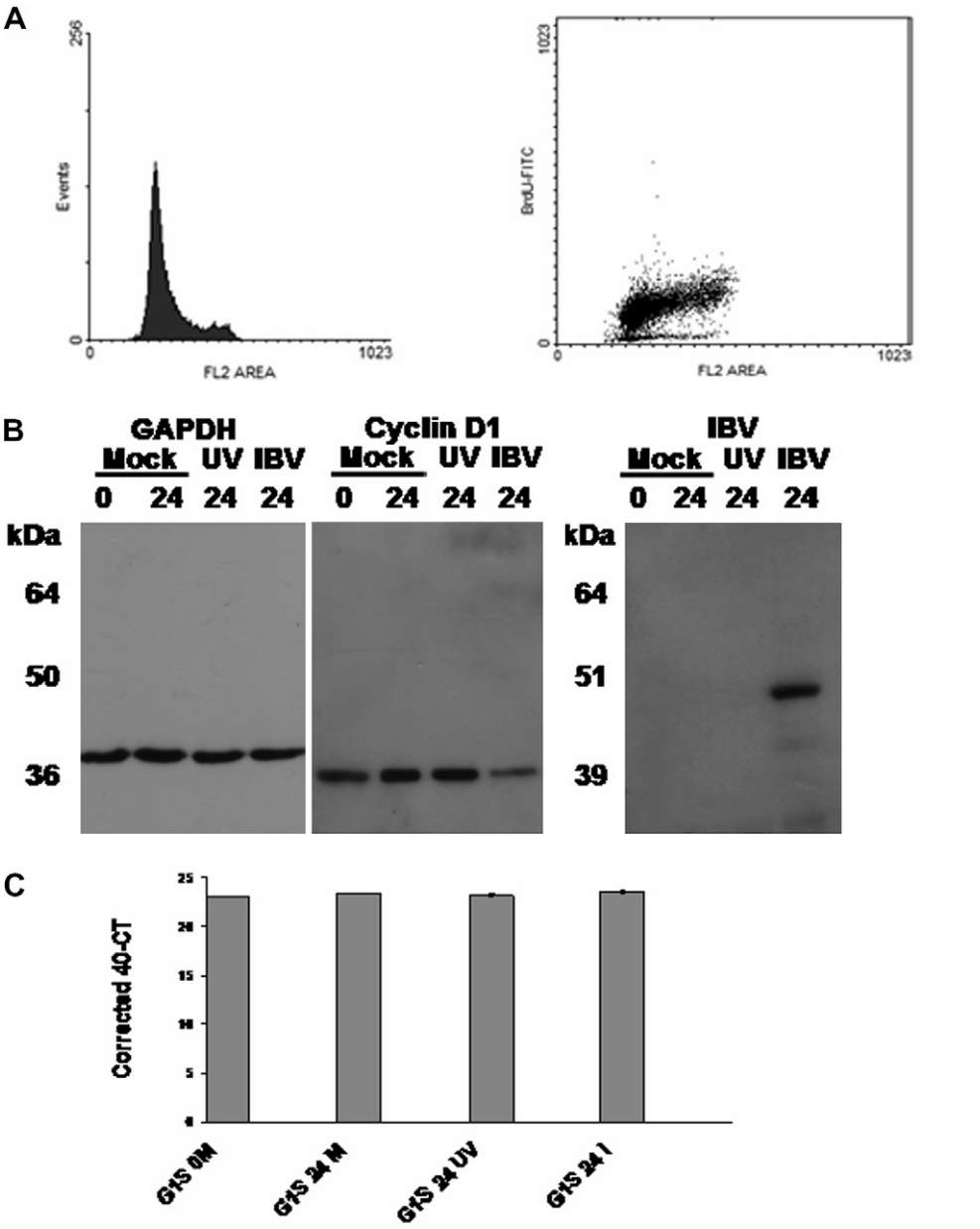

Fig. 3. (A) Propidium iodide (PI) plot and BrdU/PI staining of cell cycle profiles of cells enriched in the G1/S phase of the cell cycle using a double-T block (for the latter plot the *X*-axis is the intensity of PI staining and the *Y*-axis is the intensity of BrdU staining). (B) Western blot analysis of GAPDH, cyclin D1 and IBV proteins in mock infected cells (Mock) and cells treated with UV-inactivated virus (UV) and infectious virus (IBV) at the times indicated post-infection (h) in cells enriched in the G1/S phase of the cell cycle and then released. The migration of molecular weight markers is indicated to the left. (C) TaqMan analysis of the amount of cyclin D1 mRNA in cells enriched in the G1/S phase of the cell cycle (indicated G1S) and then released at the indicated times (h), in either mock (M) or cells infected with IBV (I) or treated with UV-inactivated virus (UV).

Variation in sampling and RNA preparation was accounted for by standardising the C_t values for gene-specific products for each sample to the C_t value of 28S rRNA product for the same sample. RNA levels between samples in the same experiment were normalised by pooling values from all samples in that experiment and calculating the mean C_t value for 28S rRNA-specific gene product. Variations in each individual 28S rRNA sample compared to the mean were then calculated. Differences in input of total RNA were calculated by determining the slope of the 28S rRNA $\log_{10}$ dilution series regression line. Using the slopes of the respective gene specific or 28S rRNA $\log_{10}$ dilution series regression lines, the difference in input total RNA, as represented by the 28S rRNA, was then used to adjust the gene specific C_t values [25].

This was done as follows:

$$\text{Corrected } C_t \text{ value} = C_t + (N_t - C_t')^* S/S'$$

where C_t is the mean sample C_t; N_t is the experimental 28S mean; C_t' is the mean 28S of sample; S is the IBV 5′ UTR/IBV 3′UTR slope; and S' is the 28S slope.

Results were then expressed as 40-C_t values.

2.9. Analysis of the sub-cellular localisation of native cyclin D1

Confocal sections were captured using a Zeiss LSM 510 Meta laser scanning confocal microscope [26]. Native cyclin D1 was labelled with rabbit anti cyclin D1 (1:200, Santa Cruz) and detected with either goat anti rabbit FITC (1:200, Sigma) (green) or chicken anti rabbit Texas Red (1:200, Sigma) (red). Where appropriate, IBV-infected cells were fixed post-infection and IBV proteins were labelled with chicken anti-IBV polyclonal sera (1:200, Charles River) and detected with rabbit anti chicken antibody conjugated to AlexaFluor633 (Molecular

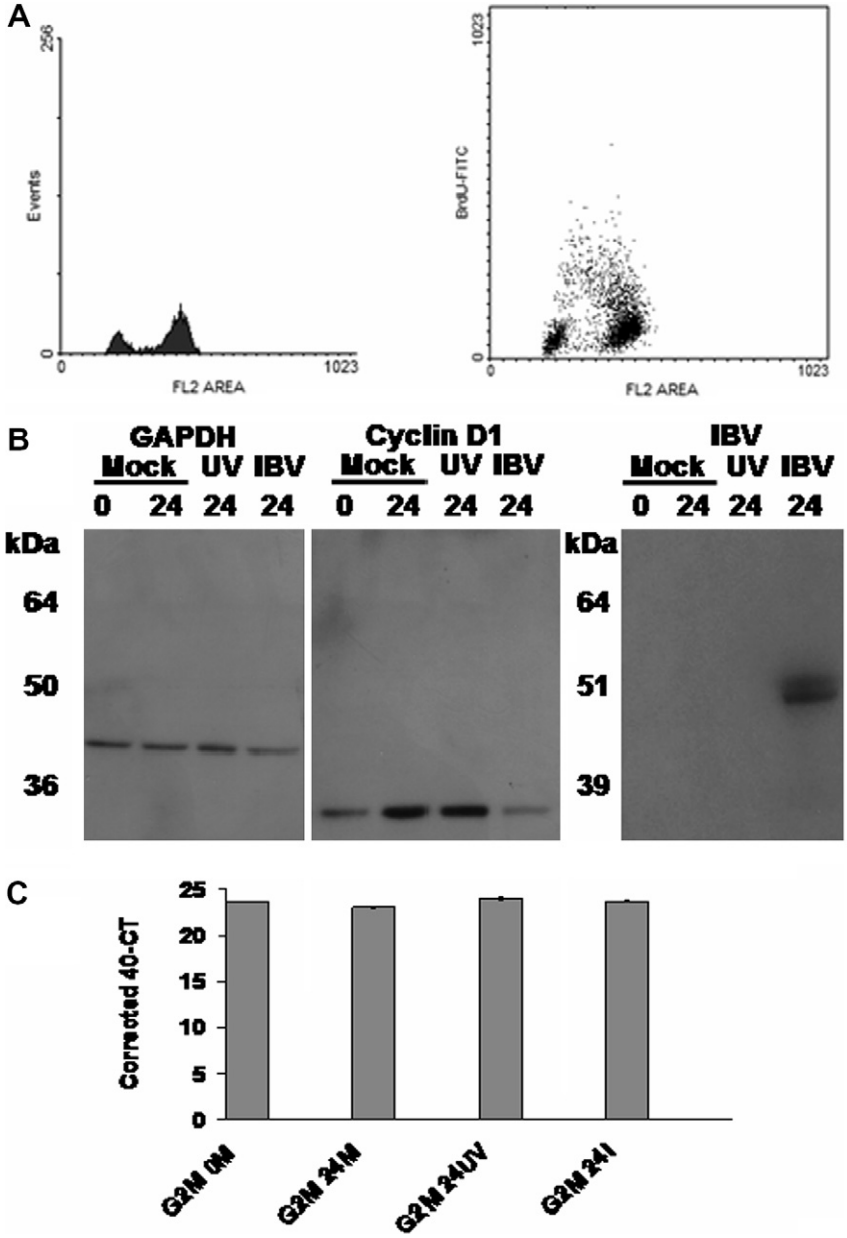

Fig. 4. (A) Propidium iodide (PI) plot and BrdU/PI staining of cell cycle profiles of cells enriched in the G2/M phase of the cell cycle using nocodazole (for the latter plot the *X*-axis is the intensity of PI staining and the *Y*-axis is the intensity of BrdU staining). (B) Western blot analysis of GAPDH, cyclin D1 and IBV proteins in mock infected cells (Mock) and cells treated with UV-inactivated virus (UV) and infectious virus (IBV) at the times indicated post-infection (h) in cells enriched in the G2/M phase of the cell cycle and then released. The migration of molecular weight markers is indicated to the left. (C) TaqMan analysis of the amount of cyclin D1 mRNA in cells enriched in the G2/M phase of the cell cycle (indicated G2M) and then released at the indicated times (h), in either mock (M) or cells infected with IBV (I) or treated with UV-inactivated virus (UV).

Probes/Invitrogen 1:200) (far red). Images were scanned four times. No cross talk between channels was determined by switching off the appropriate excitation laser and imaging the corresponding emission. In cells co-transfected with pEGFP-IBVN and pECFP-cyclin D1 the respective fusion proteins were analyzed by meta-confocal microscopy [21,27].

3. Results and discussion

To determine whether the reduction of cyclin D1 protein was caused by replicating virus or as a cellular response to the presence of virus particles, the amount of cyclin D1 protein from IBV infected or UV-inactivated virus treated cells was compared to that of mock-infected cells (Fig. 1A). Densitometric analysis indicated there was an approximately 14-fold reduction in the level of cyclin D1 protein in IBV-infected cells compared to either mock-infected or cells treated with UV-inactivated virus (data not shown). This data are in contrast to the retrovirus, HIV, and DNA virus, cytomegalovirus, which can cause cell cycle perturbations in the absence of replicating virus [28,29]. UV-inactivation of IBV was determined by Western blot analysis to detect viral proteins (Fig. 1A) and RT-PCR to viral RNA (data not shown). No viral RNA or their products were detected in cells treated with UV-inactivated virus.

Real-time RT-PCR (TaqMan) was used to quantify the amount of cyclin D1 mRNA between mock-infected, UV-inactivated virus treated and IBV-infected cells. Total RNA was prepared from the three separate experiments and cyclin D1 mRNA from each sample analyzed in triplicate. Representative data from one experiment is shown (Fig. 1B). There was no significant difference in the level of cyclin D1 mRNA

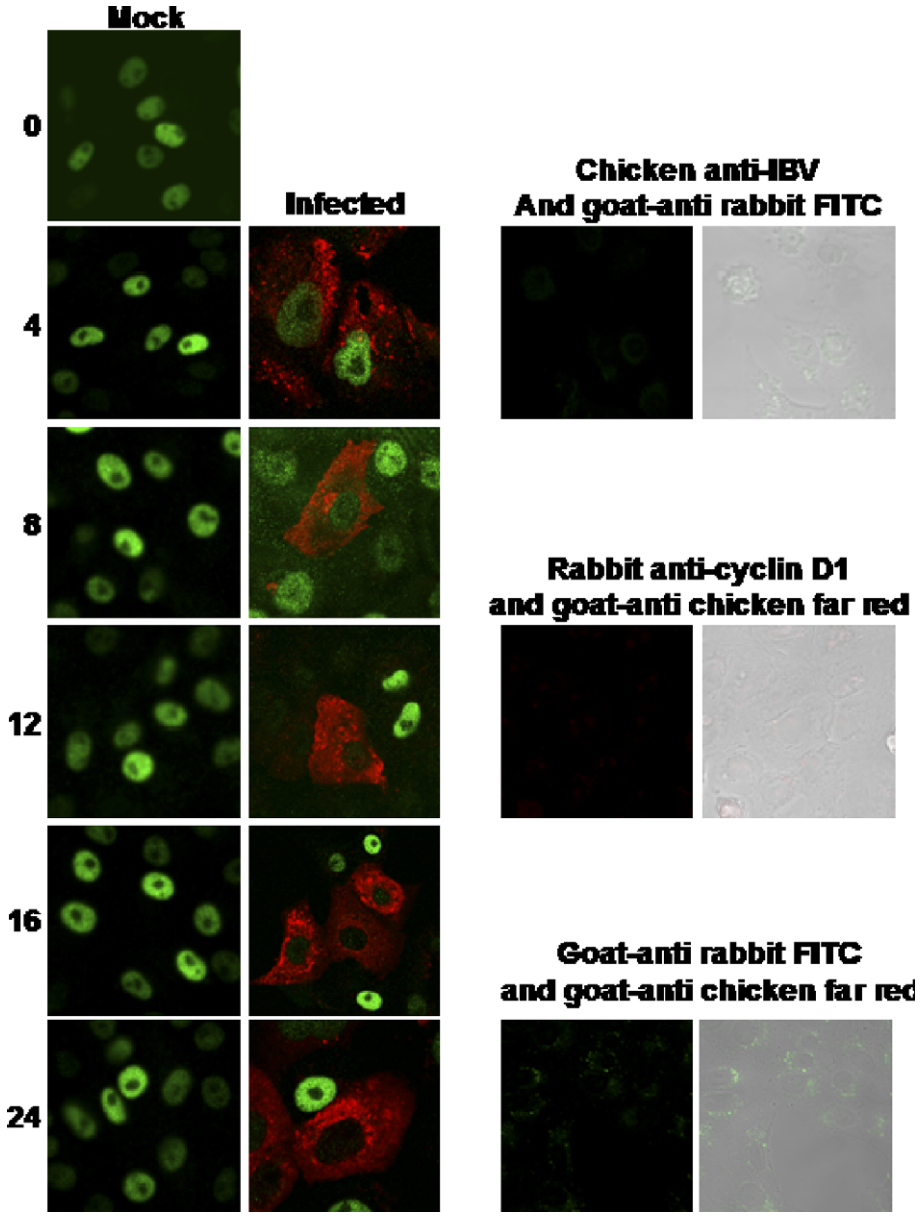

Fig. 5. Confocal microscopy analysis of the sub-cellular localisation of cyclin D1 (green) in mock and IBV-infected (red) asynchronously replicating cells at the times indicated post-infection. Antibody controls are also presented with the corresponding transmission phase contrast images.

between each population, suggesting the reduction of cyclin D1 in IBV-infected cells is post-transcription. To confirm that real-time RT-PCR could distinguish between different levels of RNA, the amount of virus RNA was assayed at 0, 1, 4, 8, 12 and 24 h pi, using primer and probe sets to detect viral genomic RNA. The results indicated that there was an approximately 8-fold increase in viral genomic RNA between 1 and 24 h post-infection (each 40-C_t value indicates a twofold difference) (Table 1) and demonstrated that real-time RT-PCR can distinguish changes in RNA levels.

Although IBV will infect dividing cells one of the major targets of infection is the upper epithelial cell layer [30] which contains quiescent cells in the G0 phase of the cell cycle. In order to model this, Vero cells were enriched in the G0 phase of the cell cycle by serum starvation which was confirmed by flow cytometry [6] (Fig. 2A), resulting in an average of 87% of cells in the G0 phase, 10% in the S phase and 3% in the G2/M phase of the cell cycle. This compared to non-confluent asynchronously growing cells, in which an average of 58% of cells are in G0/G1, 38% in S phase and 4% in the G2/M phase (data not shown and [6]). The cells were then simultaneously released and treated with either UV-inactivated virus or infected with IBV and the levels of cyclin D1 protein (determined by Western blot) and mRNA (determined by TaqMan as per above) compared to that of mock-infected cells at 24 h post-infection and release. The data indicated that the amount of cyclin D1 protein was reduced in IBV infected cells compared to mock-infected or UV-inactivated virus treated cells (Fig. 2B). However, the level of cyclin D1 mRNA was not significantly different for cells either treated with IBV or UV-inactivated virus or left untreated (Fig. 2C). However, there was an approximately fourfold increase (two 40-C_t values) in cyclin D1 mRNA in these cells compared to cells at 0 h (Fig. 2C), which may reflect an increase in mRNA and protein synthesis due to entry into the cell cycle.

Cyclin D1 mainly functions during the G1 phase and at the G1/S phase transition before being rapidly degraded via the ubiquitin pathway during S phase [17]. Cyclin D1 levels then begin to rise again in the G2/M phase. Therefore, we investigated the effect on cyclin D1 mRNA and protein in IBV-infected cells which had been enriched at either the G1/S or G2/M phase border. Vero cells were enriched in these phases

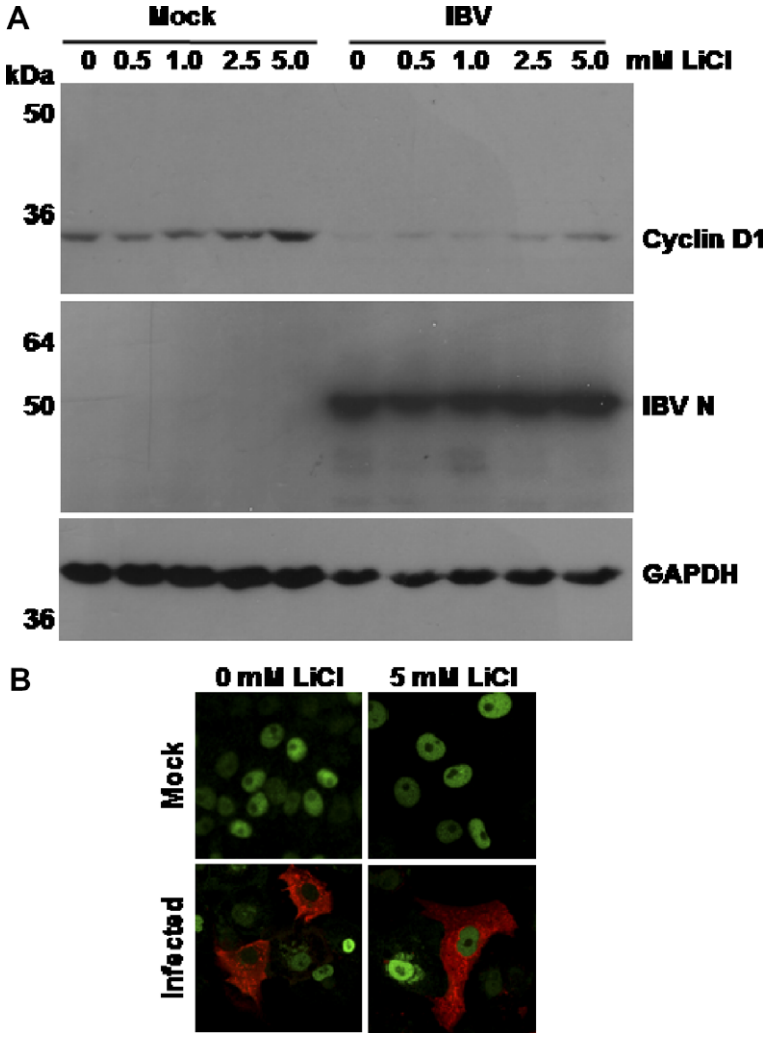

Fig. 6. (A) Western blot analysis of cyclin D1, IBV and GAPDH proteins in mock-infected or virus infected (IBV) cells treated with various of concentrations of LiCl (indicated). The data shown is one of three separate experiments which had identical results. (B) Confocal microscopy analysis of the sub-cellular localisation of cyclin D1 (green) in mock and IBV-infected (red) asynchronously replicating cells treated with 0 and 5 mM LiCl.

using, either a double thymidine block or nocodazole treatment [6]. After treatment, cell cycle profiles were determined using dual flow cytometry and the data indicated that the cells had been enriched at the G1/S or G2/M phase border (Figs. 3A and 4A, respectively). For double thymidine treated cells there were an average of 88% of cells in the G1 phase, 3% in S phase and 9% in the G2/M phase, and in cells treated with nocodazole, there were an average of 20% of cells in G1, 23% in S phase and 57% in the G2/M phase, as described previously [6]. The cells were then simultaneously released and treated with either UV-inactivated virus or infected with IBV and the levels of cyclin D1 protein (determined by Western blot) and mRNA (determined by TaqMan as per above) compared to that of mock-infected cells at 24 h post-infection and release. The data indicated that the amount of cyclin D1 protein was reduced in IBV-infected cells compared to mock-infected or UV-inactivated virus treated cells for both cell cycle conditions (Figs. 3B and 4B). There was no significant difference in the levels of cyclin D1 mRNA for both conditions (Figs. 3C and 4C). This mirrored the observations of cyclin D1 protein and mRNA in asynchronously growing and G0 enriched Vero cells, and indicated that reduction in cyclin D1 levels by IBV was not dependent on the cell cycle stage at the time of infection. Interestingly, in the cells enriched in the G2/M phase of the cell cycle whilst the amount of cyclin D1 protein was greater in mock-infected cells at 24 h post-infection compared

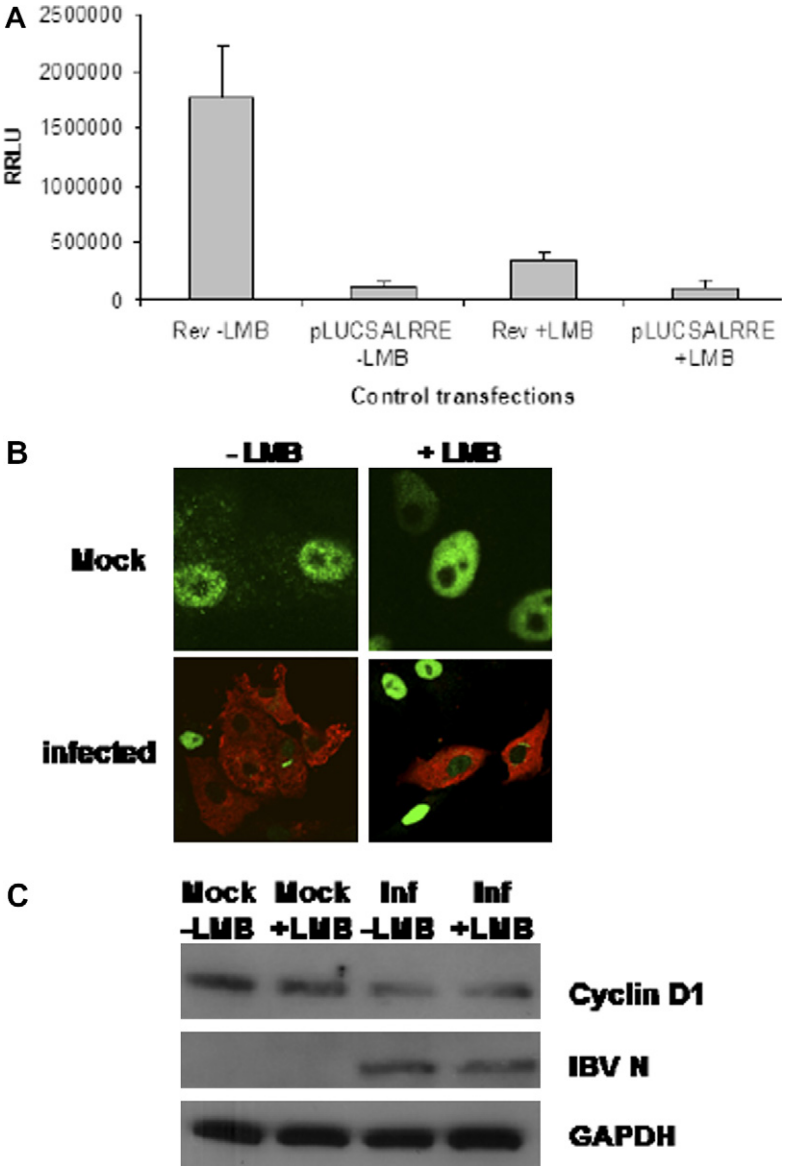

Fig. 7. (A) Histogram showing the activity of LMB in relation to its effect to inhibit CRM1 mediated export of HIV-1 Rev protein. The first and third columns are where the luciferase reporter RNA construct is expressed in combination with the HIV-1 Rev protein (plasmid pRev, denoted Rev). Whereas the second column and fourth columns are where the luciferase reporter RNA construct (plasmid pLUCSALRRE) is expressed in the absence of the HIV-1 Rev protein. The third and fourth columns is data from LMB positive cells (indicated +LMB) whereas the first and second column is data derived from cells not treated with LMB (indicated −LMB). (B) Confocal microscopy analysis of cyclin D1 (green) in mock-infected and IBV-infected (red) asynchronously replicating cells either untreated or treated with LMB. (C) Western blot analysis of cyclin D1, IBV and GAPDH proteins in mock-infected or IBV-infected asynchronously replicating cells either untreated or treated with LMB.

to 0 h, in infected cells the amount of cyclin D1 remained unchanged compared to that at 0 h. This result could be attributed to the fact that in uninfected cycling cells cyclin D1 is rapidly degraded in S phase and then increases again in the G2 phase [31], whereas IBV arrests cells in the early G2 phase of the cell cycle [6] and therefore cyclin D1 levels may not have started to increase.

Previous Western blot data indicated that cyclin D1 protein levels were significantly reduced in infected cells by 24 h post-infection [6]. Immunofluoresence analysis of cyclin D1 in infected cells indicated that cyclin D1 protein was less than in mock-infected cells from 4 h post-infection and was absent from the nucleus by 24 h post-infection, reflecting the Western blot analysis (Fig. 5). However, at early time points there are insufficient cells infected to distinguish cyclin D1 changes by Western blot analysis. Therefore, to study the degradation of cyclin D1 protein by Western blot analysis coupled to confocal microscopy time points post-16 h infection were utilised.

In replicating cells, cyclin D1 can be phosphorylated on Thr286 by glycogen synthase kinase 3 beta (GSK3β) promoting nuclear export and subsequent degradation in the cytoplasm [32,33]. However, cyclin D1 can also be exported for degradation independently of GSK3β via unknown mechanisms [34]. To distinguish between these two possibilities, cells were either mock or infected with IBV and then treated at 8 h post-infection with varying concentrations of LiCl, which have been shown to decrease GSK3β activity [35].

Western blot analysis was used to detect cyclin D1, IBV and GAPDH proteins. The data indicated that the amount of cyclin D1 protein was greater in LiCl treated mock-infected cells compared to IBV-infected cells (Fig. 6A) and this was reflected in the accumulation of nuclear cyclin D1 as revealed immunofluoresence analysis (Fig. 6B). Increasing concentrations of LiCl resulted in a dose dependent increase in the amount of cyclin D1 protein in both mock and infected cells. This indicated that there was a population of cyclin D1 whose nuclear export was GSK3β dependent. However, in IBV infected LiCl treated cells the amount of cyclin D1 was less than in mock-infected cells and therefore indicated that a population of cyclin D1 was still being targeted for degradation.

Cyclin D1 is exported from the nucleus to the cytoplasm via the exportin CRM-1 [36,37]. To test whether this was the case in IBV-infected cells, mock and infected cells were treated with the CRM-1 inhibitor, leptomycin B (LMB). To confirm that the LMB treatment was active in these experiments, an RNA export assay was used based on the export of HIV-1 REV that utilizes the CRM1 pathway [19]. A luciferase gene was placed within an inefficiently spliced intron that contained the REV response element (creating plasmid pLUCSALRRE). The pre-mRNA is normally retained in the nucleus and the exported, spliced mRNA lacks the luciferase gene. Export is facilitated through co-expressing HIV-1 Rev protein under the control of a CMV promoter (plasmid pRev), which ensures that the pre-mRNA is actively exported through the CRM1 pathway and luciferase activity would therefore be detected. The presence of LMB would inhibit the REV-dependent mRNA export, confirming that LMB treatment of cells was effectively blocking the CRM1-dependent export pathway. Therefore, in order to assess the activity of LMB Vero cells were transfected with pLUCSALRRE with or without LMB and also in the absence and presence of pRev (Fig. 7A). The data indicated that in the absence of pRev there was no significant difference in luciferase activity between LMB treated or untreated cells, and this level was taken as background activity. In contrast, when the pRev protein was present, the level of luciferase was 70% less in LMB treated cells compared to untreated cells, indicating that LMB reduced CRM1-mediated export.

Immunofluoresence analysis indicated that in mock-infected cells in the presence or absence of LMB cyclin D1 was retained in the nucleus (Fig. 7B). Whereas in the presence of LMB in infected cells cyclin D1 was observed in the nucleus, although to a lesser extent. (Fig. 7B). The stabilising affect of LMB on cyclin D1 in infected cells was confirmed by Western blot analysis (Fig. 7C).

To test whether degradation of cyclin D1 in virus infected cells was mediated via the cellular proteosomal pathway cells were either mock or infected with IBV or treated with UV-inactivated virus, and then treated 8 h post-infection with the proteosomal inhibitor MG132. This inhibitor has been used to investigate ubiquitin mediated degradation of cyclin D1 in

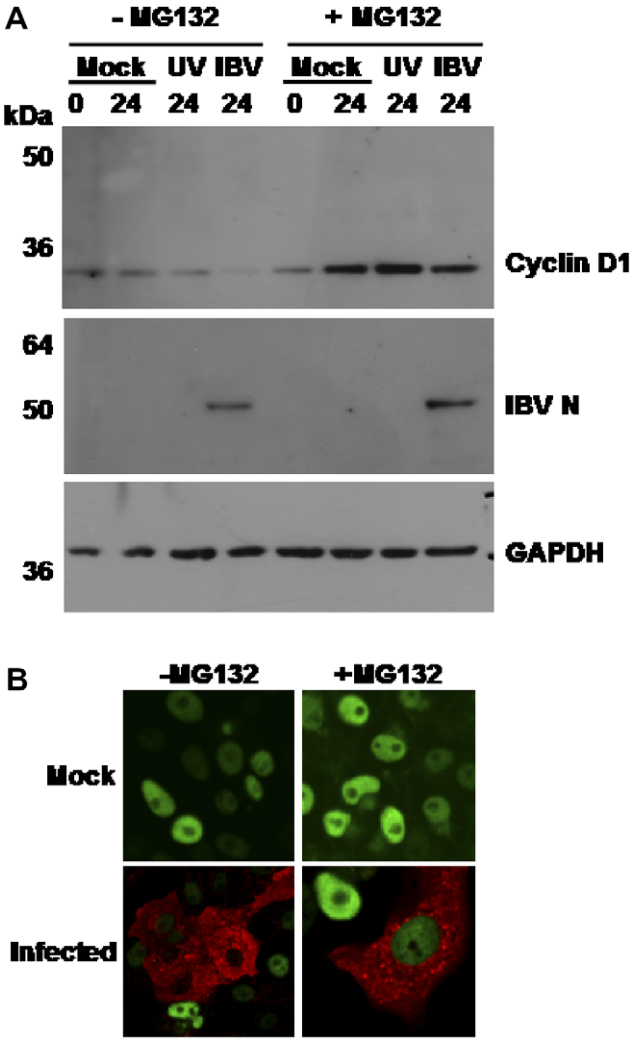

Fig. 8. (A). Western blot analysis of cyclin D1, IBV N and GAPDH proteins in mock (M) and virus infected (I) or cells treated with UV-inactivated virus (UV) at 24 h post-infection. Treatment MG132 is denoted (+) and untreated (−). (B) Confocal microscopy analysis of cyclin D1 (green) in mock-infected and IBV-infected (red) asynchronously replicating cells either untreated or treated with MG132.

coxsackie virus infected cells [38]. Western blot analysis was used to detect cyclin D1, GAPDH and IBV proteins. The data indicated more cyclin D1 protein in MG132 treated cells compared to untreated (Fig. 8A), which was confirmed by immunofluoresence analysis of both mock and infected cells in the presence and absence of MG132 (Fig. 8B). This indicated that in both mock and IBV infected cells the degradation of cyclin D1 was dependent on the cellular proteosomal pathway. However, as the amount of cyclin D1 in IBV infected cells was less than in mock infected cells treated with MG132 there may be a population of cyclin D1 that is being degraded via an unknown mechanism. In the presence of 5 mM LiCl and 10 μM MG132 cyclin D1 levels were part stabilised in IBV infected cells as revealed by both Western blot and immunofluoresence analysis (Fig. 9A and B, respectively) (although there as variation on a cell to cell basis indicated by immunofluoresence).

Although the treatment of infected cells with LiCl, MG132 or LMB results in the increased stabilisation of cyclin D1 compared to untreated infected cells, there is still less cyclin D1 than when compared to mock-infected treated cells, indicating that a viral protein and/or signalling pathway may be responsible for the export of cyclin D1 from the nucleus to the cytoplasm for its subsequent degradation. One candidate viral protein, could be the IBV N protein which can traffic between the nucleolus and the cytoplasm [22,26] and interactions with the nucleolus and its proteins may be one mechanism by which RNA viruses can disrupt the cell cycle [39]. IBV N protein is a phospho-protein which binds RNA with high affinity [40,41]. In the case of the severe acute respiratory syndrome coronavirus (SARS-CoV), N protein has been shown to interact with cyclin D1 in cells expressing N protein [12]. To investigate whether IBV N protein could interact with cyclin D1 co-localisation studies using confocal microscopy and pull down studies were performed. However, no co-localisation was observed in cells expressing IBV N protein tagged to the fluorescent fusion protein, EGFP (Fig. 10A). This may have been due to the fact that IBV N protein localises principally to the cytoplasm and nucleolus, rather than the nucleus [26,42], which is in contrast to cyclin D1 which is predominately nuclear, therefore the two molecules could not interact. To test this hypothesis a mutant EGFP-tagged N protein was used in which the nuclear export signal had been deleted and whose localisation was nuclear and nucleolar [26]. However, no co-localisation was observed (Fig. 10B). Likewise, cyclin D1 was tagged N-terminally with ECFP, which resulted in the accumulation of the fusion protein predominately in the cytoplasm. Transfection of cells with this plasmid and also expressing EGFP-IBV N protein indicated that no co-localisation was observed between these two proteins in the cytoplasm (Fig. 10C).

No interaction was also found with a biochemical pull down of cell extracts using a recombinant his-tagged N protein [40,43] anchored to a solid matrix as a target (data not shown). Whereas as a control N protein could pull down the tumour suppressor protein p53 (Fig. 10D) which we have shown previ-

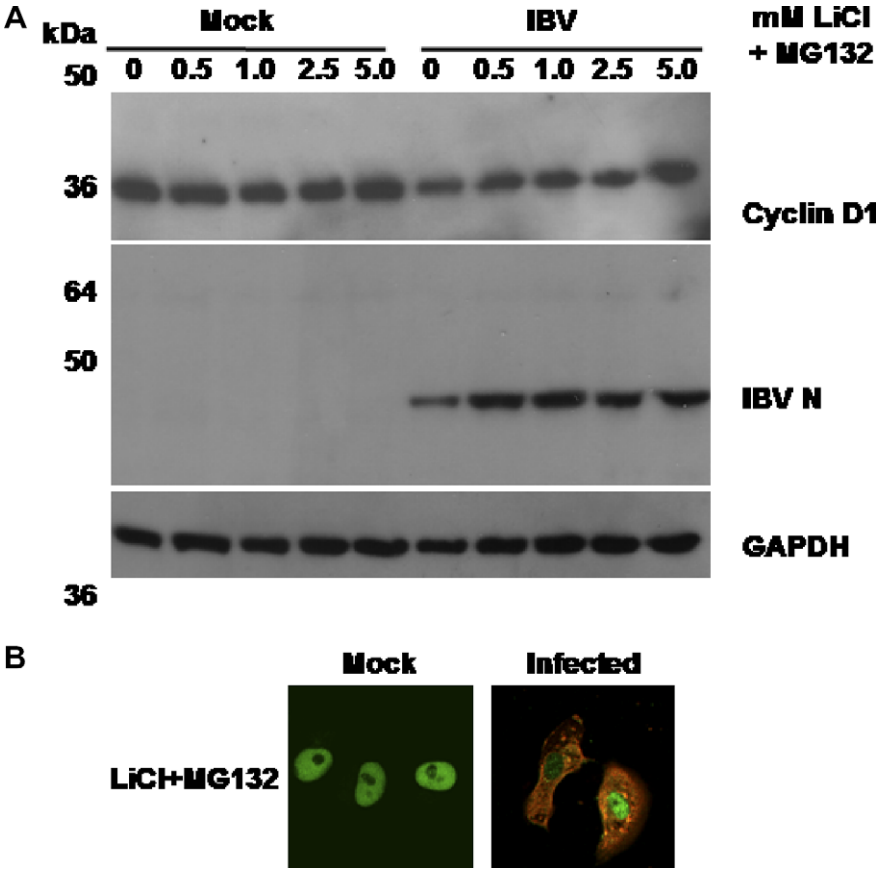

Fig. 9. (A) Western blot analysis of cyclin D1, IBV N and GAPDH proteins in mock (M) and virus-infected (I) asynchronously replicating cells at 24 h post-infection treated with LiCl (at the concentrations indicated) and with 10 uM MG132. (B) Confocal microscopy analysis of cyclin D1 (green) in mock-infected and IBV-infected (red) asynchronously replicating cells treated with 5 mM LiCl and 10 uM MG132.

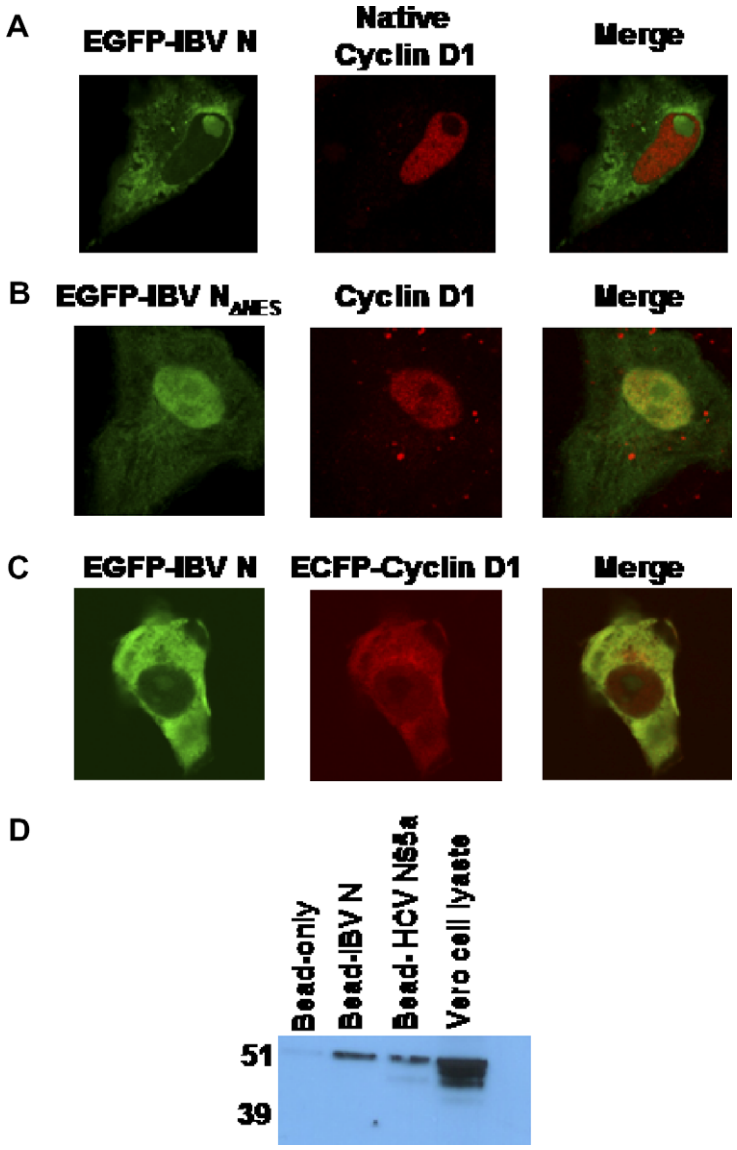

Fig. 10. Confocal microscopy analysis of the sub-cellular localisation of cyclin D1 (red) and (A) EGFP-IBV N protein and (B) EGFP-IBV $N_{\Delta NES}$ (both green). (C) Confocal microscopy analysis of the sub-cellular localisation of EGFP-IBV N protein (green) and ECFP-cyclin D1 (false coloured red). (D) Western blot analysis of pull down analysis of the tumour suppressor protein, p53, using either bead only controls, recombinant IBV N protein, the hepatitis C virus NS5a protein as a positive control, and total cell protein extract. Molecular weight markers are indicated to the left.

ously co-localises with N protein [44]. Likewise IBV N protein co-localises with and can pull down nucleolin [15,26]. The possibility remains that other viral proteins could direct the trafficking of cyclin D1 from the nucleus to the cytoplasm.

This study demonstrated that actively replicating IBV is required to decrease cyclin D1 and that this change is regulated post-transcription. This may be mediated by the arrest in the G2 phase of the cell cycle of infected cells prior to the stage when cyclin D1 levels would usually begin to rise. Furthermore, in infected cells cyclin D1 is redistributed from the nucleus to the cytoplasm, where we hypothesize it is targeted for degradation, by a viral protein dependent trafficking pathway. However, the precise mechanism of this pathway remains to be determined.

Acknowledgements: This work was funded by the award of BBSRC project grant (No. BBS/B/03416) to J.A.H. and G.B., and a BBSRC DTA/CASE studentship with Intervet UK, Ltd. to J.A.H.

References

[1] Harper, J.V. and Brooks, G. (2005) The mammalian cell cycle: an overview in: Cell Cycle Control: Mechanisms and Protocols (Humphrey, T. and Brooks, G., Eds.), pp. 113–153, Humana Press Inc., New Jersey.
[2] Guertin, D.A., Trautmann, S. and McCollum, D. (2002) Cytokinesis in eukaryotes. Microbiol. Mol. Biol. Rev. 66, 155–178.
[3] Pines, J. (1999) Four-dimensional control of the cell cycle. Nature Cell Biol. 1, 73–79.
[4] Op De Beeck, A. and Caillet-Fauquet, P. (1997) Viruses and the cell cycle (Meijer, L., Guidet, S. and Philippe, M., Eds.), Progress in Cell Cycle Research, Vol. 3, pp. 1–19, Plenum Press, New York.
[5] Cavanagh, D. (1997) *Nidovirales*: a new order comprising *Coronaviridae* and *Arteriviridae*. Arch. Virol. 142, 629–633.
[6] Dove, B.K., Brooks, G., Bicknell, K.A., Wurm, T. and Hiscox, J.A. (2006) Cell cycle perturbations induced by infection with the coronavirus infectious bronchitis virus and their effect on virus replication. J. Virol. 80, 4147–4156.
[7] Chen, C.J. and Makino, S. (2004) Murine coronavirus replication induces cell cycle arrest in G0/G1 phase. J. Virol. 78, 5658–5669.

[8] Chen, C.J., Sugiyama, K., Kubo, H., Huang, C. and Makino, S. (2004) Murine coronavirus nonstructural protein p28 arrests cell cycle in G0/G1 phase. J. Virol. 78, 10410–10419.
[9] Chau, T.N. et al. (2004) SARS-associated viral hepatitis caused by a novel coronavirus: report of three cases. Hepatology 39, 302–310.
[10] Yuan, X. et al. (2006) SARS coronavirus 7a protein blocks cell cycle progression at G0/G1 phase via the cyclin D3/pRb pathway. Virology 346, 74–85.
[11] Yuan, X., Shan, Y., Zhao, Z., Chen, J. and Cong, Y. (2005) G0/G1 arrest and apoptosis induced by SARS-CoV 3b protein in transfected cells. Virol. J. 2, 66.
[12] Surjit, M., Liu, B., Chow, V.T. and Lai, S.K. (2006) The nucleocapsid protein of severe acute respiratory syndrome-coronavirus inhibits the activity of cyclin–cyclin-dependent kinase complex and blocks S phase progression in mammalian cells. J. Biol. Chem. 281, 10669–10681.
[13] Timani, K.A. et al. (2005) Nuclear/nucleolar localization properties of C-terminal nucleocapsid protein of SARS coronavirus. Virus Res. 114, 23–34.
[14] Wurm, T., Chen, H., Britton, P., Brooks, G. and Hiscox, J.A. (2001) Localisation to the nucleolus is a common feature of coronavirus nucleoproteins and the protein may disrupt host cell division. J. Virol. 75, 9345–9356.
[15] Chen, H., Wurm, T., Britton, P., Brooks, G. and Hiscox, J.A. (2002) Interaction of the coronavirus nucleoprotein with nucleolar antigens and the host cell. J. Virol. 76, 5233–5250.
[16] Stacey, D.W. (2003) Cyclin D1 serves as a cell cycle regulatory switch in actively proliferating cells. Curr. Opin. Cell Biol. 15, 158–163.
[17] Harper, J.V. and Brooks, G. (2006) The eukaryotic cell cycle in: Viruses and the Nucleus (Hiscox, J.A., Ed.), pp. 25–68, John Wiley & Sons, Ltd., Chichester.
[18] Alonso-Caplen, F.V., Matsuoka, Y., Wilcox, G.E. and Compans, R.W. (1984) Replication and morphogenesis of avian coronavirus in Vero cells and their inhibition by monensin. Virus Res. 1, 153–167.
[19] Williams, B.J., Boyne, J.R., Goodwin, D.J., Roaden, L., Hautbergue, G.M., Wilson, S.A. and Whitehouse, A. (2005) The prototype gamma-2 herpesvirus nucleocytoplasmic shuttling protein, ORF 57, transports viral RNA through the cellular mRNA export pathway. Biochem. J. 387, 295–308.
[20] Reed, M.L., Dove, B.K., Jackson, R.M., Collins, R., Brooks, G. and Hiscox, J.A. (2006) Delineation and modelling of a nucleolar retention signal in the coronavirus nucleocapsid protein. Traffic 7, 833–848.
[21] You, J.-H. et al. (2005) Sub-cellular localisation of the severe acute respiratory syndrome coronavirus nucleocapsid protein. J. Gen. Virol. 86, 3303–3310.
[22] Reed, M.L., Howell, G., Harrison, S.M., Spencer, K.A. and Hiscox, J.A. (2007) Characterisation of the nuclear export signal in the coronavirus infectious bronchitis virus nucleocapsid protein. J. Virol., doi:10.1128/JVI.02239-0.
[23] Bicknell, K.A., Brooks, G., Kaiser, P., Chen, H., Dove, B.K. and Hiscox, J.A. (2005) Nucleolin is regulated both at the level of transcription and translation. Biochem. Biophys. Res. Commun. 332, 817–822.
[24] Kaiser, P., Underwood, G. and Davison, F. (2003) Differential cytokine responses following Marek's disease virus infection of chickens differing in resistance to Marek's disease. J. Virol. 77, 762–768.
[25] Harrison, S.M., Tarpey, I., Rothwell, L., Kaiser, P. and Hiscox, J.A. (in press). Lithium chloride inhibits the coronavirus infectious bronchitis virus in cell culture. Avian Pathol, doi:10.1080/03079450601156083.
[26] Reed, M., Dove, B.K., Jackson, R.M., Collins, R., Brooks, G. and Hiscox, J.A. (2006) Delineation and modelling of a novel nucleolar retention signal in the coronavirus nucleocapsid protein. Traffic 7, 833–849.
[27] You, J.H., Reed, M.L., Dove, B.K. and Hiscox, J.A. (2006) Three-dimensional reconstruction of the nucleolus using meta-confocal microscopy in cells expressing the coronavirus nucleoprotein. Adv. Exp. Med. Biol. 581, 313–318.
[28] Goh, W.C., Rogel, M.E., Kinsey, CM., Michael, S.F., Fultz, P.N., Nowak, M.A., Hahn, B.H. and Emerman, M. (1998) HIV-1 Vpr increases viral expression by manipulation of the cell cycle: a mechanism for selection of Vpr in vivo. Nat. Med. 4, 65–71.
[29] Lu, M. and Shenk, T. (1999) Human cytomegalovirus UL69 protein induces cells to accumulate in Gi phase of the cell cycle. J. Virol. 73, 676–683.
[30] Cavanagh, D. and Naqi, S. (1997) Infectious bronchitis in: Diseases of Poultry (Calnek, B.W., Barnes, H.J., Beard, C.W., Reid, W.M. and Yoda, H.W., Eds.), pp. 511–526, Iowa State University Press, Ames.
[31] Stacey, D.W. (2003) Cyclin D1 serves as a cell cycle regulatory switch in actively proliferating cells. Curr. Opin. Cell Biol. 15, 158–163.
[32] Guo, Y., Yang, K., Harwalkar, J., Nye, J.M., Mason, D.R., Garrett, M.D., Hitomi, M. and Stacey, D.W. (2005) Phosphorylation of cyclin D1 at Thr 286 during S phase leads to its proteasomal degradation and allows efficient DNA synthesis. Oncogene 24, 2599–2612.
[33] Diehl, J.A., Cheng, M., Roussel, M.F. and Sherr, C.J. (1998) Glycogen synthase kinase-3beta regulates cyclin D1 proteolysis and subcellular localization. Genes Dev. 12, 3499–3511.
[34] Diehl, J.A., Zindy, F. and Sherr, C.J. (1997) Inhibition of cyclin D1 phosphorylation on threonine-286 prevents its rapid degradation via the ubiquitin–proteasome pathway. Genes Dev. 11, 957–972.
[35] Stambolic, V., Ruel, L. and Woodgett, J.R. (1996) Lithium inhibits glycogen synthase kinase-3 activity and mimics wingless signalling in intact cells. Curr. Biol. 6, 1664–1668.
[36] Benzeno, S. and Diehl, J.A. (2004) C-terminal sequences irect cyclin D1-CRM1 binding. J. Biol. Chem. 279, 56061–56066.
[37] Alt, J.R., Cleveland, J.L., Hannink, M. and Diehl, J.A. (2000) Phosphorylation-dependent regulation of cyclin D1 nuclear export and cyclin D1-dependent cellular transformation. Genes Dev. 14, 3102–3114.
[38] Luo, H. et al. (2003) Ubiquitin-dependent proteolysis of cyclin D1 is associated with coxsackievirus-induced cell growth arrest. J. Virol. 77, 1–9.
[39] Hiscox, J.A. (2007) RNA viruses: hijacking the dynamic nucleolus. Nat. Rev. Microbiol. 5, 119–127.
[40] Chen, H., Gill, A., Dove, B.K., Emmett, S.R., Kemp, F.C., Ritchie, M.A., Dee, M. and Hiscox, J.A. (2005). in: Mass spectroscopic characterisation of the coronavirus infectious bronchitis virus nucleoprotein and elucidation of the role of phosphorylation in RNA binding using surface plasmon resonance J. Virol. 79, 1164–1179.
[41] Spencer, K.A. and Hiscox, J.A. (2006) Characterisation of the RNA binding properties of the coronavirus infectious bronchitis virus nucleocapsid protein aminoterminal region. FEBS Lett. 580, 5993–5998.
[42] Hiscox, J.A., Wurm, T., Wilson, L., Cavanagh, D., Britton, P. and Brooks, G. (2001) The coronavirus infectious bronchitis virus nucleoprotein localizes to the nucleolus. J. Virol. 75, 506–512.
[43] Chen, H., Coote, B., Attree, S. and Hiscox, J.A. (2003) Evaluation of a nucleoprotein-based enzyme-linked immunosorbent assay for the detection of antibodies against infectious bronchitis virus. Avian Path. 32, 519–526.
[44] Dove, B.K., You, J.-H., Reed, M.L., Emmett, S.R., Brooks, G. and Hiscox, J.A. (2006) Changes in nucleolar architecture and protein profile during coronavirus infection. Cell. Microbiol. 8, 1147–1157.